

# High-Frequency Nanofluidics: An Experimental Study using Nanomechanical Resonators

D. M. Karabacak, V. Yakhot, and K. L. Ekinci\*

Department of Aerospace and Mechanical Engineering,  
Boston University, Boston, Massachusetts, 02215

(Dated: May 26, 2019)

Here we apply nanomechanical resonators to the study of oscillatory fluid dynamics. A high-resonance-frequency nanomechanical resonator generates a rapidly oscillating flow in a surrounding gaseous environment; the nature of the flow is studied through the flow-resonator interaction. Over the wide frequency ( $100 \text{ kHz} \leq \omega/2\pi \leq 100 \text{ MHz}$ ) and pressure ( $25 \text{ Torr} \leq p \leq 1000 \text{ Torr}$ ) range explored, we observe signs of a transition from Newtonian to non-Newtonian flow at  $\omega\tau \approx 1$ , where  $\tau$  is a properly defined fluid relaxation time. The obtained experimental data is in close quantitative agreement with a theory that predicts purely elastic fluid response as  $\omega\tau \rightarrow \infty$ .

The Navier-Stokes equations based upon the Newtonian approximation have been remarkably successful over the centuries in formulating solutions for relevant flow problems both in bulk and near solid walls [1]. The Newtonian approximation breaks down, however, when the particulate nature of the fluid becomes significant to the flow. The Knudsen number,  $Kn = \lambda/L$ , is one parameter, which is commonly used to settle whether the Newtonian approximation can be applied to a medium or not. Here, one compares the mean free path  $\lambda$  in the medium to an *ill-defined* characteristic length  $L$ . A second defining parameter, especially for oscillatory flow, is the Weissenberg number,  $Wi = \tau/T$ , which compares the characteristic time scale  $T$  of the flow with the relaxation time  $\tau$  in the medium. As  $\tau/T = \omega\tau$  is varied — for instance, by varying the flow frequency  $\omega$  or the relaxation time  $\tau$  — the nature of the flow changes drastically.

Recent developments in nanometer scale engineering have created a subfield of fluid dynamics called nanofluidics [2]. Most nanofluidics work is concerned with flow in nanoscale channels and remains strictly in the Newtonian regime. In contrast, emerging nanometer scale mechanical resonators [3–5], with frequencies already extended into the microwaves [6, 7], offer an uncharted parameter space for studying nanofluidics. For a high-frequency nanomechanical resonator with resonance frequency  $\omega/2\pi$ , one can tune  $\omega\tau$  over a wide range — in fact, possibly reaching the limits of the Newtonian approximation in a given liquid or gas. This not only allows experimental probing of a flow regime that was inaccessible by past experiments [8–12], but also presents the unique prospect of designing nanodevices for key technological applications.

To complement the recent theoretical interest in high frequency nanofluidics [2, 13–15], we experimentally studied the interaction of high-frequency nanomechanical

resonators with a gaseous environment. The gaseous environment presents an ideal fluid for these studies, where one can effectively tune  $\tau$  by changing the pressure  $p$ . On the other hand, varying the resonator dimensions changes the mechanical resonance frequency  $\omega/2\pi$ . When combined, the two experimental parameters allow  $\omega\tau$  to be varied over several orders of magnitude effectively.

In order to cover a broad frequency range, we fabricated doubly-clamped beam resonators of sub-micron scale cross-sections and micron scale lengths from silicon [16]. We also employed commercial microcantilevers to further extend the frequency range. For the measurements, we used a pressure-controlled optical characterization chamber connected to a high purity  $N_2$  source. The resonators were actuated electrostatically and their displacements were measured optically [16]. The measurements were performed under linear drive; moreover, the results remained independent of the rms displacement amplitudes of 1–10 nm — as confirmed by Michelson interferometry.

Figure 1 depicts the typical resonant response of a nanomechanical resonator as the background  $N_2$  pressure in the chamber is increased. Both the decrease in the resonance frequency and the broadening of the lineshape result from the resonator-gas interaction. The frequency shift is due to the mass loading from the boundary layer, while the broadening is a manifestation of the energy dissipation in the fluid. In other words, mass loading and dissipation arise from the respective in-phase and out-of-phase motion of the surrounding fluid in relation to the resonator motion. The analysis can be simplified by using a one-dimensional damped harmonic oscillator approximation [17],  $\ddot{x} + \gamma\dot{x} + \omega^2x = f/m$ , where  $f/m$  represents the force per unit effective mass of the resonator. The quality factor  $Q$ , which is a comparison of the stored energy to the dissipated energy per cycle, is related to  $\gamma$  as  $\gamma \approx Q/\omega$ . Here, we extracted both the resonance frequency  $\omega/2\pi$  and  $Q$  using nonlinear least squares fits to the Lorentzian response function of the resonator. In addition, for low- $Q$  (high pressure), we verified the Lorentzian fit results through fits to the real

\*Author to whom correspondence should be addressed. Electronic mail: ekinci@bu.edu

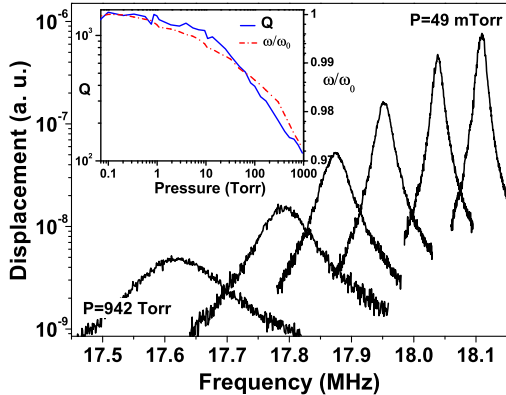


FIG. 1: Resonance of a silicon doubly-clamped beam of width  $w = 500$  nm, length  $l = 13$   $\mu\text{m}$  and thickness of  $h = 280$  nm at various  $\text{N}_2$  pressures in the chamber:  $p = 0.049, 5.4, 32, 100, 302$  and  $942$  Torr. The inset shows the extracted quality factor  $Q$  and normalized resonance frequency  $\omega/\omega_0$  of the same device as a function of pressure.

and imaginary components of the complex transmission [18]. Typical changes in  $\omega$  and  $Q$  of a nanomechanical resonator during a pressure sweep are shown in the inset of Fig. 1. Both  $\omega$  and  $Q$  approach their respective intrinsic values,  $\omega_0$  and  $Q_0$ , at low pressure.

Before presenting further results, we must clarify the nature of the fluidic energy dissipation. The motion of the fluid with respect to the solid boundary creates a complex, position-dependent shear stress on the resonator surface. The inertial and dissipative components of the net shear force are proportional to the displacement and the velocity, respectively. For a single device, as the parameters are changed, the fluidic dissipation can be characterized by either the fluidic quality factor  $Q_f$  given by  $Q_f^{-1} = Q^{-1} - Q_0^{-1}$  or the fluidic dissipation  $\gamma_f = \omega/Q_f$ . To compare different devices with different sizes and geometries, one needs to further realize that the fluidic dissipation is proportional to the effective surface area  $S_{\text{eff}}$ , while the stored energy in the resonator is proportional to the effective mass  $m$  [27]. With this naive assumption, we define a normalized fluidic dissipation,  $\gamma_n = \gamma_f m/S_{\text{eff}}$ . We note in passing that the uncertainty in, and subsequently the pressure range for the dissipation measurements are set by  $Q_0$ . Typical  $Q_0 \sim 10^3$  and experimental uncertainty of 5% limited our range of accurate fluidic dissipation measurements to  $p > 10$  Torr.

The normalized fluidic dissipation  $\gamma_n$  observed in three resonators with different sizes and frequencies are presented in Fig. 2(a),(b) and (c) as a function of gas pressure. The 78 kHz device is a commercial micro-cantilever. A change in the slope is noticeable for the data in (a), and (b) at approximate pressures of 1 and 300 Torr, respectively. The turn points marked in the plots correspond to  $\omega\tau \approx 1$ , and is discussed in detail below. For the high-

est frequency beam at 102 MHz shown in (c), the turn point falls outside the available pressure range. Molecular flow model [14], which takes into account specular collisions, fits our data only at the ideal gas limit, i.e., at low pressure. Note that a multiplicative constant of 0.9 was used in all three to improve the fits. Viscous effects [19, 20] and squeeze-film effects [21, 22], commonly observed in MEMS, did not introduce significant damping for the small high-frequency devices up to atmospheric pressure.

The solid lines in Fig. 2 are fits to the theory by Yakhut and Colosqui [13] developed from the Boltzmann Equation in the relaxation time approximation. After imposing the no-slip boundary condition and geometric normalization, this theory [13] culminates in the expression

$$\gamma_n \approx \frac{1}{(1 + \omega^2 \tau^2)^{3/4}} \sqrt{\frac{\omega \mu \rho_f}{2}} \left[ (1 + \omega \tau) \cos\left(\frac{\tan^{-1} \omega \tau}{2}\right) - (1 - \omega \tau) \sin\left(\frac{\tan^{-1} \omega \tau}{2}\right) \right]. \quad (1)$$

In Eq. 1,  $\gamma_n$  is expressed in terms of the viscosity  $\mu$ , the density  $\rho_f$  and the effective relaxation time  $\tau$  of the fluid, and the frequency  $\omega$  of the resonator. The only unavailable parameter is the relaxation time  $\tau$ . In order to obtain the fits, we assumed that  $\tau$  satisfied the empirical form,  $\tau \propto 1/p$  [12, 23]. The key prediction of the Yakhut-Colosqui [13] theory is that the turn point in  $\gamma_n$  occurs when  $\tau \approx 1/\omega$ . Thus our experiments provided a direct and unique way to extract  $\tau$  as a function of pressure  $p$ : Fig. 2(d) displays the experimentally extracted  $\tau$  from the transition points of 12 resonators as a function of pressure. Through linear fitting, one can obtain the expression  $\tau \approx 1850/p$  [in units of nanoseconds when  $p$  is in units of Torr]. The end result of this exercise is the set of fits in Fig. 2. To improve all the fits in Fig. 2, the results emerging from Eq. 1 with the appropriate material properties and  $\tau$  were multiplied by 2.8. In general, all our data sets could be fit adequately using Eq. 1 after multiplying by  $2.8 \pm 0.7$ .

The fluidic dissipation in individual resonators shown in Fig. 2 suggests that there, indeed, is a transition marked by  $\omega\tau \approx 1$ . By changing the pressure in the experiment, we effectively tune the parameter  $\tau$ . Further support for the transition at  $\omega\tau \approx 1$  comes from extended measurements in the frequency parameter space. Figure 3(a) and (b) show  $\gamma_n$  from devices spanning a huge frequency range plotted against the intrinsic frequency  $\omega_0$  of the resonators at four different pressures. Note that Fig. 3(a) is a logarithmic plot, while Fig. 3(b) is a linear plot emphasizing the high frequency portion of the data. This comparison between different devices with different sizes is possible only after normalization of the dissipation data by the factor  $S_{\text{eff}}/m$  [28]. The solid lines in Fig. 3 are fits using Eq. 1; the  $\tau$  at each pressure

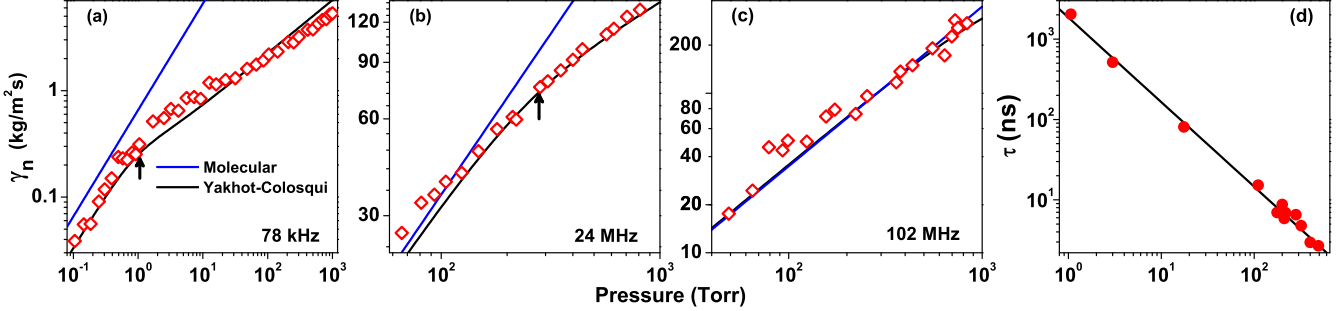


FIG. 2: Normalized fluidic dissipation  $\gamma_n$  as a function of pressure for (a) a cantilever with dimensions ( $w \times h \times l$ )  $53 \times 2 \times 460$   $\mu\text{m}$ , and nanomechanical doubly-clamped beams with dimensions of (b)  $230 \text{ nm} \times 200 \text{ nm} \times 9.6 \mu\text{m}$  (c)  $390 \text{ nm} \times 200 \text{ nm} \times 3.6 \mu\text{m}$ . Resonance frequencies are as indicated and the approximate turning points are marked with arrows. The lines are fits to molecular collision model [14] and Eq. 1 using  $\tau \approx 1850/p$  [13]. The molecular collision and the Yakhot-Colosqui predictions were multiplied by 0.9 and 2.8, respectively, for *all* resonators. (d) Relaxation time  $\tau$  as a function of pressure. The points were extracted from fluidic dissipation data sets, such as those shown in (a) and (b), of 12 resonators. The solid line is a least-mean-squares fit and indicates that  $\tau \approx 1850/p$ .

was obtained from  $\tau \approx 1850/p$ . The apparent transition points correspond to  $\omega\tau \approx 1$ , this time shown on the frequency axis. Again, we have multiplied all the fits by 2.8 as in Fig. 2; we estimate that the multiplicative constant arises from the nature of the complex distributed motion of the resonator as well as the approximate surface-to-volume normalization that we have adopted. We stress again that the results displayed here are independent of the amplitude of motion. The agreement between theory and experiment is remarkable.

Returning to Fig. 1, a small decrease in the resonance frequency is also apparent as the pressure is increased. While increased damping causes a decrease in the resonance frequency, this down-shift is negligible in our measurements. The observed decrease is primarily due to the mass of the fluid layer that is being displaced in phase with the resonator. The mass  $m_f$  of the fluid layer can be determined as  $\frac{\Delta\omega}{\omega_0} \approx \frac{m_f}{2m}$  [5]. For the purpose of analyzing the experimental data, we make the following two approximations:  $w, h \ll \delta$  and  $\frac{m_f}{m} \approx \frac{\rho_f \delta^2}{\rho_s w h}$ , where  $\delta$  represents the boundary layer thickness, and  $\rho_f$  and  $\rho_s$  are the fluid and solid densities, respectively. Thus,  $\delta$  can be extracted experimentally. In Fig. 4, we plot  $\delta$  as a function of pressure for four beams of *identical* widths ( $w = 500$  nm) and thicknesses ( $h = 280$  nm) but *varying* lengths and resonance frequencies. First,  $\delta \propto \sqrt{1/\omega}$  — in qualitative agreement with the Stokes result [1]. However, there appears to be an inconsistency as  $\delta \propto 1/p^{1/3}$ . We note that the Yakhot-Colosqui theory [13] underestimates the frequency shift.

The transition observed in our experiments can be interpreted in most general terms as follows. The simple linear relation between stress and rate-of-strain in a Newtonian fluid breaks down at high frequencies. The Boltzmannian theory developed by Yakhot and Colosqui suggests that this result is independent of the fluid. In

fact, these results should be equally valid in dense liquids as in rarefied gases. This transition at  $Wi = \omega\tau \approx 1$  was described [13] as a “viscoelastic to elastic” transition owing to the fact that the waves generated in the fluid by the resonator motion do *not* decay as  $\omega \rightarrow \infty$ . Our results also suggest that there is some universality with respect to device geometry: both in cantilevers and doubly-clamped beams, the same naive geometric normalization resulted in a consistent analysis. Finally, the transition point allowed for the extraction of an empirical correlation between  $\tau$  and  $p$ .

There is a relentless effort to develop nanomechanical resonators operating in gaseous [24] and liquid environments [25]. Our results should impact the design of next-generation nanomechanical resonators. Figure 3 suggests that fluidic dissipation saturates at high frequencies. Take, for instance, two doubly-clamped beam resonators with identical widths and thicknesses but different lengths, i.e., identical  $\frac{S_{eff}}{m} \approx \frac{1}{w} + \frac{1}{h}$  but different frequencies such that  $\omega_1 < \omega_2$ . If  $\omega_1 < \omega_2 < 1/\tau$ , the ratio of the quality factors of the two resonators in fluid becomes  $\frac{Q_{2f}}{Q_{1f}} \sim \sqrt{\frac{\omega_2}{\omega_1}}$ . On the other hand, if  $\omega_1 < 1/\tau < \omega_2$ , then  $\frac{Q_{2f}}{Q_{1f}} \sim \omega_2 \sqrt{\frac{\tau}{\omega_1}}$ . Finally, for  $1/\tau < \omega_1 < \omega_2$ ,  $\frac{Q_{2f}}{Q_{1f}} \sim \frac{\omega_2}{\omega_1}$ . This observation suggests that the shorter, higher-frequency resonator will always be more resilient in a given fluid but the degree of resilience depends upon the fluid  $\tau$ . Yet, for two devices with identical frequencies, the smaller one with the larger  $\frac{S_{eff}}{m}$  will have the lower  $Q_f$ . For a scaling problem where both  $\frac{S_{eff}}{m}$  and device frequency increase, the nature of the scaling determines the end result. Finally, the surface roughness, especially for very small devices, is expected to have an important role in nanofluidics of nanomechanical resonators [26].

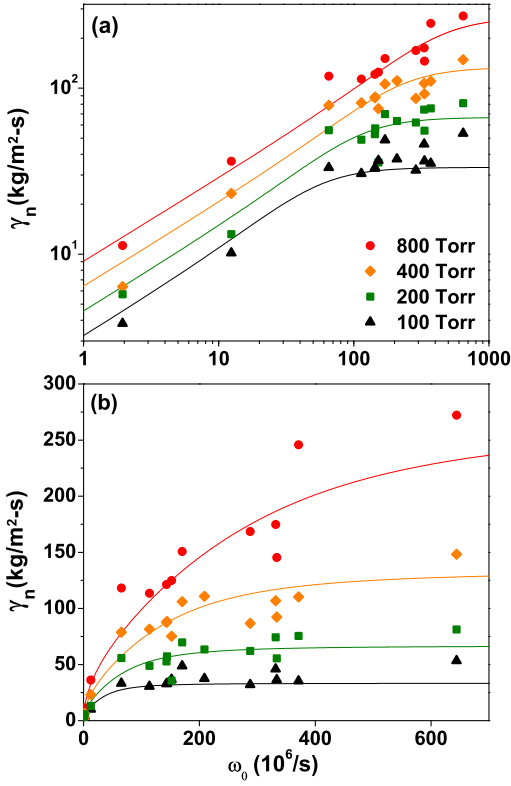


FIG. 3: (a) Normalized fluidic dissipation  $\gamma_n$  as a function of the resonator frequency  $\omega_0$  for several resonators at four different pressures. From top to bottom,  $\tau \approx 2.3, 4.6, 9.2, 18.5$  ns. The lines are fits calculated using Eq. 1. All the predictions were multiplied by the same fitting factor of 2.8 (also see Fig. 2). (b) The same data shown in a linear plot to emphasize the high frequency portion.

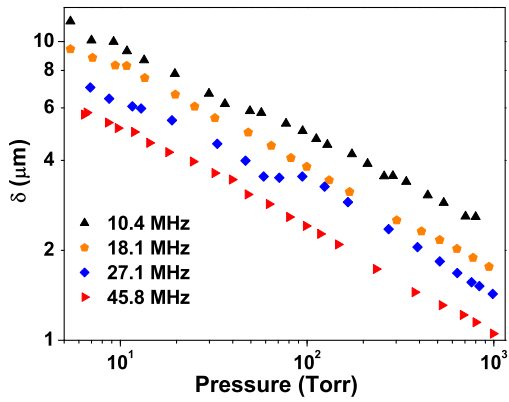


FIG. 4: Estimated boundary layer thickness  $\delta$  as a function of pressure for four doubly-clamped nanomechanical beams of identical widths  $w = 500$  nm and thickness  $h = 280$  nm, but varying resonance frequencies.

We thank M. Paul and R. Bhiladvala for helpful conversations. We acknowledge generous support from NSF through grant Nos. CMS-324416 and BES-216274.

---

- [1] E. M. Lifshitz and L. D. Landau, *Fluid Mechanics* (Butterworth-Heinemann, Oxford, 1987), 2nd ed.
- [2] G. Karniadakis, A. Beskok, and N. Aluru, *Microflows and Nanoflows* (Springer, New York, 2005), 1st ed.
- [3] M. L. Roukes, *Sci. Amer. Sept.*, 42 (2001).
- [4] H. G. Craighead, *Science* **290**, 1532 (2000).
- [5] K. L. Ekinci and M. L. Roukes, *Rev. of Sci. Instr.* **76**, 1101 (2005).
- [6] X. M. H. Huang, C. A. Zorman, M. Mehregany, and M. L. Roukes, *Nature* **421**, 496 (2003).
- [7] H. B. Peng, C. W. Chang, S. Aloni, T. D. Yuzvinsky, and A. Zettl, *Phys. Rev. Lett.* **97**, 087203 (2006).
- [8] J. T. Tough, W. D. McCormick, and J. G. Dash, *Phys. Rev.* **132**, 2373 (1963).
- [9] L. Bruschi and M. Santini, *Rev. of Sci. Instr.* **46**, 1560 (1975).
- [10] P. I. Oden, G. Y. Chen, R. A. Steele, R. J. Warmack, and T. Thundat, *Appl. Phys. Lett.* **68**, 3814 (1996).
- [11] Y. Xu, J.-T. Lin, B. W. Alphenaar, and R. S. Keynton, *Appl. Phys. Lett.* **88**, 143513 (2006).
- [12] M. Rodahl, F. Hook, A. Krozer, P. Brzezinski, and B. Kasemo, *Rev. of Sci. Instr.* **66**, 3924 (1995).
- [13] V. Yakhot and C. Colosqui (2006), URL [arXiv.org:nl1n/0609061](http://arXiv.org:nl1n/0609061).
- [14] R. B. Bhiladvala and Z. J. Wang, *Phys. Rev. E* **69**, 036307 (2004).
- [15] M. R. Paul and M. C. Cross, *Phys. Rev. Lett.* **92**, 235501 (2004).
- [16] T. Kouh, D. Karabacak, D. H. Kim, and K. L. Ekinci, *Appl. Phys. Lett.* **86**, 013106 (2005).
- [17] A. Cleland, *Foundations of Nanomechanics* (Springer, New York, 2003), 1st ed.
- [18] P. J. Petersan and S. M. Anlage, *J. Appl. Phys.* **84**, 3392 (1998).
- [19] J. E. Sader, *J. Appl. Phys.* **84**, 64 (1998).
- [20] F. R. Blom, S. Bouwstra, M. Elwenspoek, and J. H. J. Fluitman, *J. Vac. Sci. Technol. B* **10**, 19 (1992).
- [21] J. L. T. Veijola, H. Kuusima and T. Ryhanen, *Sensors and Actuators A* **48**, 239 (1995).
- [22] J. J. Belch, *J. of Lubrication Theory* **105**, 615 (1983).
- [23] E. T. Watts, J. Krim, and A. Widom, *Phys. Rev. B* **41**, 3466 (1990).
- [24] M. Li, H. X. Tang, and M. L. Roukes, *Nature Nanotechnology* **2**, 114 (2007).
- [25] S. Verbridge, L. Bellan, J. Parpia, and H. Craighead, *Nano Letters* **6**, 2109 (2006).
- [26] G. Palasantzas, *Appl. Phys. Lett.* **90**, 041914 (2007).
- [27] The typical mass loading in these experiments is small. Thus both the frequency and the effective mass can be taken as constant for all practical purposes.
- [28]  $S_{eff} \approx 2l(w + h)$ ;  $m \approx Clwh\rho$ ; the value of  $C$  depends upon the structure geometry and the mode shape. A distributed force approximation for calculating  $C$  was appropriate for our experimental conditions.